26^{th} *EPS Conf. on Contr. Fusion and Plasma Physics, Maastricht, 14 - 18 June 1999   ECA Vol.23J (1999) 525 - 528*

MHD Stability Analysis of Reversed Magnetic Shear Discharges in the HL-2A Tokamak †

Qingdi Gao, R.V. Budny,* Jinhua Zhang, Hongpeng Qu, and Zhenggui Xiao

Southwestern Institute of Physics, P O Box 432, Chengdu 610041, P R China
**Princeton Plasma Physics Laboratory, Princeton university, NJ08543, USA*

1. Introduction

The HL-2A tokamak under construction (R=1.6m, a=0.32-0.4m, κ=1.0-1.3, δ=0.0-0.5, B_T=2.8T, I_p=0.48MA)[1] is based upon the ASDEX load assembly which was transferred from IPP, Garching to SWIP, Chengdu in 1996. One of the HL-2A objectives is to study enhanced core plasma confinement using current profile control. Recent studies [2,3] revealed many favorable properties of plasma configurations with reversed magnetic shear (RS). The experimental observation of greatly reduced transport in RS plasmas provides a strong motivation to further explore current profile control by which optimized RS operation may be established and maintained for timescales beyond the characteristic current diffusion time. It is noted that the recent experiments of RS plasmas were transient in nature, so it is important to understand the MHD properties of RS discharges. In the HL-2A tokamak, the various schemes of auxiliary heating and current drive, including NBI (3MW), ICRH (1MW), LHCD (2.5MW), and ECRH (0.5MW), will be combined with the device flexibility to optimize the current profile. In this paper we model realistic RS discharges in HL-2A using the TRANSP code. After establishing self-consistent RS equilibria, we carry out stability analysis for some typical plasma configurations including ones with peaked pressure profile equilibria and significant bootstrap current fractions.

2. Shear reversal formation with NBI heating

The time dependent TRANSP code [4] is used to simulate RS operation in HL-2A. The simulated discharge is an easily-controlable deuterium discharge with the plasma current rising to ~0.3MA in 0.3s. Neutral beam injection (NBI) begins at a low power (0.8-1.0MW) at ~0.15s, then an additional 1.5 MW is injected. For the high NBI power phase the heat diffusivity models are extrapolated from TFTR results, with amplitudes modified to match the expected global energy confinement time. In HL-2A, the closed divertor configuration combined with divertor pumping [1] is expected to effectively screen the sputtering impurity flow during high power heating phase. Z_{eff} is assumed to be in the range generally observed in current experiments: 1.7~2.0. The plasma density is varied following specified wave-forms. As the RS plasmas develop internal transport barriers with peaked pressure profiles, the central electron density increases from $\approx 2.7\times10^{19}\,m^{-3}$ to $\approx 1.0\times10^{20}\,m^{-3}$ with a gradually peaking profile ($n_e(0)/\langle n_e\rangle$=1.7 - 3.4, where $\langle n_e\rangle$ is the volume averaged density). As the plasma β rises, the RS configuration is formed and sustained with the minimum q(q_{min}) evolving from q_{min}>3.0 to q_{min}<2.0 and q_{min} being localized at x_{min}(r_{min}/a)~ 0.3. The q profiles and

† The work is supported by China Nuclear Science Foundation under grant No Y917C0315

pressure profiles at different times are shown in Fig.1. The parameters of two typical configurations are as follows,

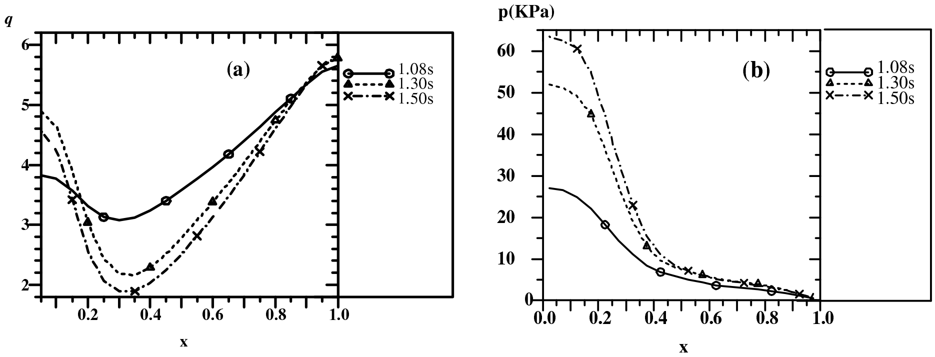

Fig.1 (a) q-profiles and (b) pressure profiles at t=1.08s, 1.30s, and 1.50s

(1) The case at t=1.08s represents a higher $q_{\rm min}$ configuration. The plasma current is I_p=265kA with bootstrap current fraction f_{BS}=0.32, and neutral beam driven current I_{NB}=35kA. The central value of the safety factor is q_0=3.81 with $q_{\rm min}$=3.08, q_ψ=5.65, and the internal inductance ℓ_i=0.65. The poloidal beta and normalized beta are, respectively, β_p=1.21 and β_N=1.45 with a pressure peaking factor of $p(0)/\langle p\rangle$=5.1, where $\langle p\rangle$ stands for the volume-averaged pressure.

(2) The case at t=1.30s is a higher bootstrap current configuration. The plasma current is the same as the pervious case, with more than half of the current driven from the bootstrap effect (f_{BS}=0.51) and ~15 percent driven by neutral beam (I_{NB}=33kA). The current profile is more hollow with q_0=4.84, $q_{\rm min}$=2.14, q_ψ=5.76 and ℓ_i=0.79. The shear reversal region is slightly wider than the previous case, with $x_{\rm min}\approx$0.32. Since the plasma density and electron temperature are increased, the beta values are higher, β_p=1.65, β_N=1.74 and $p(0)/\langle p\rangle$=5.5.

3. MHD stability for the RS equilibria with peaked pressure profile

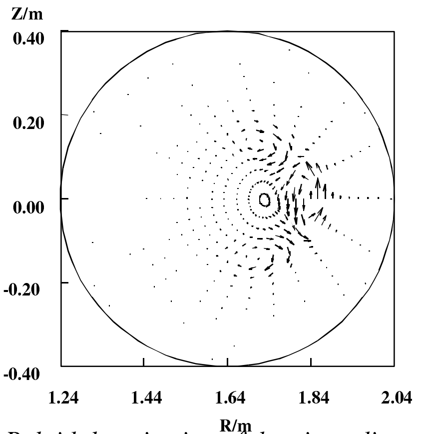

Fig.2 Poloidal projection of the eigen displacement vector (n=1.5) for the equilibrium at t=1.08s

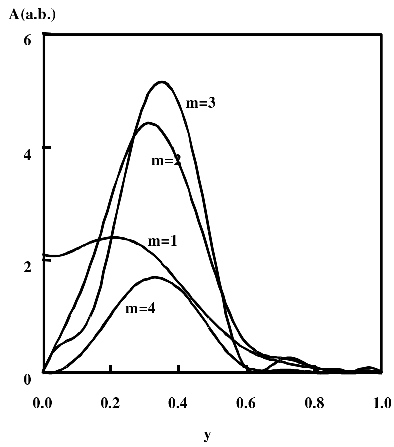

Fig.3 Poloidal harmonics of the perpendicular displacement for the instability shown in Fig.2

Peaked pressure profiles and a strong central negative shear characterize the RS configuration described above. These configurations are analyzed with respect to several MHD instability modes including low-*n* MHD modes, ballooning modes, and resistive interchange modes. The ideal MHD instability due to low-*n* modes is analyzed with the ERATO(SWIP) code. For the stability analysis, the equilibia generated with TRANSP are recalculated on a finer grid of 99 flux points and 81 poloidal points, using as input the p(ψ) (including pressure produced by the NBI energetic particles) and $\langle j_{\parallel} \rangle(\psi)$ profiles given numerically by the TRANSP results. For the RS equilibrium at t=1.08s, the low-*n* modes located at the region around $q_{\min}$ are unstable. As shown in Fig.2, the poloidal projection of the unstable displacement vector demonstrates that the strong perturbation occurs at the low shear region (around $x_{\min}$). We note that the growth rate versus *n* is of oscillatory feature, and the mode structure indicates that m=1,2,3,4 are the Fourier harmonics of the radial perturbation displacement when $nq_{\min}$ >4.0 (Fig.3). For the equilibrium at t=1.30s we also find that the unstable low-*n* modes are of an internal nature with the perturbation occurring around $x_{\min}$, while the pattern of the displacement eigenvector is different from the t=1.08s case.

To examine the ballooning stability, we integrate the ballooning mode differential equation around each flux surface for the TRANSP calculated configuration, obtaining the critical pressure gradient for the first stability of ideal ballooning modes. Comparing the critical pressure gradient with the equilibrium pressure gradient shows that the ballooning modes are stable across the whole plasma for the equilibrium at t=1.08s, as shown in Fig.4*a*. As the discharge evolving towards higher β, the pressure profile becomes more peaked with the value of the pressure gradient at t=1.30s being more than twice as high as that at t=1.08s. Even in the equilibrium with the higher peaked pressure profile, the ideal ballooning modes are still stable (Fig.4b). Due to profile differences, marginally unstable ballooning modes can occasionally occur in a small region outside $x_{\min}$ (also shown in Fig.4b), which is coincident with the RS experiment observation [5].

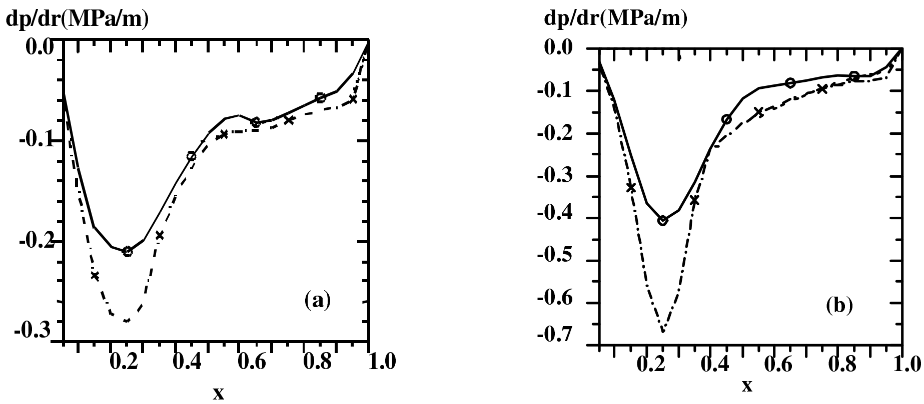

Fig.4 Critical pressure gradient for the ideal ballooning stability (dotted dash line) and actual pressure gradient (full line) for the equilibrium (a) at t=1.08s, and (b) at t=1.30s

Resistive interchange modes can be driven unstable by large pressure gradients in the reversed magnetic shear region [6]. The stability criterion for resistive interchange modes D_R<0 is related to the ideal interchange (Mercier) criterion D_I <0 through the relationship

$D_R=D_I+(H-1/2)^2$, where

$$H = \frac{m_0 p' v' g}{(2p)^2 q'}\left(\left\langle \frac{1}{|\nabla y|^2}\right\rangle - \frac{\left\langle B^2/|\nabla y|^2\right\rangle}{\left\langle B^2\right\rangle}\right), \qquad (1)$$

In the central reversed shear region, we can use the large aspect ratio expansion to obtain a simplified stability criterion for the resistive interchange modes,

$$D_s \equiv -s\left[\beta_p(r)+\ell_i(r)/2\right]-\left(1-\frac{1}{q^2}\right)<0 \qquad (2)$$

were s=rq'/q is the magnetic shear. According to Eq.(2), the conventional tokamak configurations with positive magnetic shear are inherently stable against the resistive interchange modes provided $q \geq 1$. But in the RS plasmas the resistive interchange stability criterion can be violated when the central poloidal beta is large and the shear is strongly negative. For the equilibrium at t=1.08s, the calculation indicates that interchange modes are unstable in the central negative shear region with an unstable window extending to *x*»0.2. The low-*n* MHD modes revealed by the ERATO analysis can not be interchange modes because they are located in the vicinity of shear reversal point ($x \approx 0.3$) where is not covered by the unstable window against interchange modes.

4. Summary

The TRANSP code, which has been benchmarked in many tokamak experiments, is used to model reversed magnetic shear operation anticipated in the HL-2A tokamak. The modeling indicates that the RS configurations formed by neutral beam heating are characterized by strongly peaked pressure profiles leading to high bootstrap current fractions.

MHD instability analysis against ideal low *n* modes, ideal ballooning modes, and resistive interchange modes has been carried out for the RS equilibria. The low-*n* internal modes, located in the low shear region around the minimum of *q* are unstable, showing that those modes are pressure driven instabilities. The ballooning modes are stable across the whole plasma. Nevertheless, as the profiles evolve in the RS discharge, ballooning instabilities can occur occasionally in a small area outside the shear reversal point. Due to high pressure gradients in the central negative shear region, resistive interchange instabilities arise with the unstable window not extending to low shear region.

References

1. Gao, Qingdi, and the HL-2A team, High performance operation of HL-2A and its upgrade, The First Japan-China Workshop on Improved Performance in Toroidal Plasmas (Hefei, 1997), JAERI-memo 10-020(1998)
2. Turnbull, A. D., *et al.,* Phys. Rev. Lett. 74 (1995) 718
3. Levinton, F. M., *et al.,* Phys. Rev. Lett. 75 (1995) 4417
4. Budny, R. V., *et al.,* Nucl. Fusion 35 (1995) 1497
5. Manickam, J., *et al.,* in Fusion Energy (Proc.16th Int. Conf. Montreal, 1996) Vol. 1, IAEA, Vienna (1997) 453
6. Chu, M. S., *et al.,* Phys. Rev. Lett. 77(1996) 271